Plasmon-polariton waves guided by thin lossy metal films of finite width: Bound modes of asymmetric structures

Pierre Berini*
University of Ottawa, School of Information Technology and Engineering, 161 Louis Pasteur Street, P.O. Box 450, Stn. A, Ottawa, Ontario, K1N 6N5, Canada

(Received 4 May 2000; revised manuscript received 25 October 2000; published 13 March 2001)

The purely bound electromagnetic modes of propagation supported by asymmetric waveguide structures, comprised of a thin lossy metal film of finite width on a dielectric substrate and covered by a different dielectric superstrate, have been characterized at optical wavelengths. The dispersion of the modes with film thickness and width has been assessed and the effects caused by varying the difference between the superstrate and substrate dielectric constants on the characteristics of the modes have been determined. The modes are quite different from those supported by corresponding slab structures or similar finite-width symmetric waveguides. Unlike these limiting cases, the dispersion with film thickness can exhibit an unusual oscillatory character which is explained by a switching or swapping of the constituent interface modes. In addition, the four fundamental modes supported can evolve such that none has a diminishing attenuation with diminishing film thickness. This rather complex evolution of modes is unique to asymmetric finite-width structures. Under certain conditions, a long-ranging mode having a field distribution that is suitable to excitation using an end-fire technique can be supported. The long-ranging mode has a cutoff thickness below which it is no longer propagated, and its attenuation near cutoff decreases very rapidly, much more so than the attenuation related to the long-ranging mode in a comparable symmetric waveguide. Furthermore, its cutoff thickness is larger than that of the s_b mode in the corresponding asymmetric slab waveguide, which implies that decreasing the film width increases the sensitivity of the mode to the asymmetry in the structure. This result is interesting and potentially useful in that the propagation characteristics of the mode can be affected by a smaller change in the dielectric constant of the substrate or superstrate compared with the s_b mode guided by the corresponding slab structure.

DOI: 10.1103/PhysRevB.63.125417 PACS number(s): 42.82.Et, 42.79.Gn, 78.20.Bh

I. INTRODUCTION

At optical wavelengths, the electromagnetic properties of some metals (gold, silver, and copper, for example) closely resemble those of an electron gas. Numerous experiments as well as classical electron theory yield an equivalent negative dielectric constant for many metals when excited by an electromagnetic wave at or near optical wavelengths.[1,2] It is also well known that the interface between semi-infinite materials having positive and negative dielectric constants can guide transverse magnetic (TM) surface waves. In the case of a metal-dielectric interface at optical wavelengths, these waves are termed plasmon-polariton modes and propagate as electromagnetic fields coupled to surface plasmons (surface plasma oscillations) which are comprised of conduction electrons in the metal.[3]

A metal film of a certain thickness bounded by dielectrics above and below can serve as an optical slab (infinitely wide) waveguiding structure, with the core of the waveguide being the metal film. When the film is thin enough, the plasmon-polariton modes guided by the interfaces become coupled due to field tunneling through the metal, thus creating supermodes that exhibit dispersion with metal thickness. The modes supported by infinitely wide symmetric and asymmetric metal film structures are well-known. Some notable published works include Refs. 3–10 with Burke *et al.*[5] and Yang *et al.*[8] providing a good review of surface waves in general, and metal slabs in particular.

Metal slabs are of limited practical interest since they offer one-dimensional (1D) field confinement only, with confinement provided along the vertical axis, perpendicular to the direction of wave propagation. This implies of course that optical fields spread out laterally as they propagate away from a point source used as the excitation. Metal films of finite thickness and width however, offer two-dimensional (2D) field confinement in the plane transverse to the direction of propagation. Such structures may be useful for signal transmission and routing or to construct passive components such as couplers and power splitters if suitable low-loss waveguides can be fabricated.

The purely bound mode spectrum supported by symmetric structures comprised of a thin metal film of finite width embedded in a homogeneous dielectric background has already been investigated theoretically,[11] and results suggest that mode power attenuation values near 0.1 dB/cm are achievable with even lower values being possible. Recently, propagation along straight waveguide segments of finite width has been demonstrated in an end-fire experiment, confirming the existence of these modes.[12] Interest in the modes supported by thin metal films has recently intensified due to their application in optical communications devices and components. Metal films are commonly employed in optical polarizing devices[13] while long-range surface plasmon-polaritons can be used for optical signal transmission and routing over short distances.[6,12] The need to characterize the mode spectrum of metal film waveguides of finite width is manifest and results obtained thus far suggest that the wave-

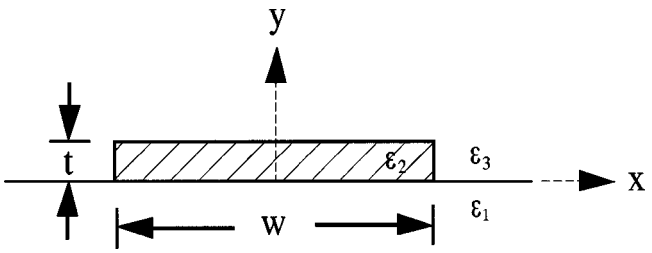

FIG. 1. Waveguide structure considered in this study. The core is comprised of a lossy metal film of thickness *t*, width *w*, and permittivity ϵ_2. The metal film is supported by a homogeneous semi-infinite substrate of permittivity ϵ_1 and the cover or superstrate is a homogeneous semi-infinite dielectric of permittivity ϵ_3.

guide may find widespread use as the basis of an integrated optics technology.

The purpose of this paper is to present a detailed description of the purely bound modes of propagation supported by asymmetric waveguiding structures comprised of a thin lossy metal film of finite width, supported by a semi-infinite homogeneous dielectric substrate and covered by a different semi-infinite homogeneous dielectric superstrate. The evolution of modes due to variations in the film's thickness and width, and in the dielectric constant of the surrounding media, are investigated. (Some preliminary results of this study have already been reported as a short communication.)[14]

The paper is organized as follows. Section II further sets the context by presenting the physical basis and solution approach used to obtain mode solutions, and by summarizing the known salient features of the purely bound modes supported by structures that represent the two limiting cases to this study: infinitely wide asymmetric metal film structures and finite-width symmetric metal film structures. Sections III and IV describe the nature, dispersion and evolution with film thickness of the purely modes supported by a metal film of finite width for small and large differences in the substrate and superstrate dielectric constants, respectively. Section V describes the dispersion of modes with film width, and Sec. VI presents the evolution of the main long-ranging mode as the structure changes from a symmetric one to an asymmetric one. Concluding remarks are given in Sec. VII.

II. PHYSICAL BASIS AND OVERVIEW OF KNOWN MODE SOLUTIONS

A. Description of the waveguide structure

The structure considered in this paper is shown in Fig. 1. It consists of a metal film of thickness *t*, width *w*, and equivalent permittivity ϵ_2, supported by a semi-infinite homogeneous dielectric substrate of permittivity ϵ_1 and covered by a semi-infinite homogeneous dielectric superstrate of permittivity ϵ_3. The Cartesian coordinate axes used for the analysis are also shown; propagation takes place along the *z* axis, which is out of the page.

It is assumed that the metal region shown in Fig. 1 can be modeled as an electron gas over the wavelengths of interest. According to classical or Drude electron theory, the complex relative permittivity of the metal region is given by the well-known plasma frequency dispersion relation:[3]

$$\epsilon_{r,2}=\left(1-\frac{\omega_p^2}{\omega^2+\nu^2}\right)-j\left(\frac{\omega_p^2\nu}{\omega(\omega^2+\nu^2)}\right), \tag{1}$$

where ω is the excitation frequency, ω_p is the electron plasma frequency, and ν is the effective electron collision frequency, often expressed as $\nu=1/\tau$ with τ defined as the relaxation time of electrons in the metal.

In this study, we are specifically interested in the case $\omega^2+\nu^2<\omega_p^2$, which yields a negative value for $\mathrm{Re}\{\epsilon_2\}$, and to the situation where all materials satisfy $|\mathrm{Re}\{\epsilon_2\}| \gg |\mathrm{Im}\{\epsilon_2\}|, \epsilon_1, \epsilon_3$. These inequalities are generally respected if the metal is noble and the wavelength of interest is in the visible or infrared ranges. This class of structure holds much promise for device applications.

B. Electromagnetic wave and field equations

The modes supported by the structure illustrated in Fig. 1 are obtained by solving a suitably defined boundary value problem based on Maxwell's equations written in the frequency domain for a lossy inhomogeneous isotropic medium. Uncoupling Maxwell's equations yields the following time-harmonic vectorial wave equations for the **E** and **H** fields:

$$\nabla\times\nabla\times\mathbf{E}-\omega^2\epsilon(x,y)\mu\mathbf{E}=0, \tag{2}$$

$$\nabla\times\epsilon(x,y)^{-1}\nabla\times\mathbf{H}-\omega^2\mu\mathbf{H}=0, \tag{3}$$

where the permittivity ϵ is a complex function of cross-sectional space, describing the waveguide structure. For the structures analyzed in this paper, μ is homogeneous and taken as the permeability of free space μ_0. A time dependence of the form $e^{j\omega t}$ is implied.

The boundary value problem is solved numerically by applying the method of lines (MoL). The MoL is a well-known numerical technique and its application to various electromagnetic problems, including optical waveguiding, is well established.[15] The MoL is rigorous, accurate and flexible. It can handle a wide variety of waveguide geometries, including the structures at hand. The method is not known to generate spurious or non-physical modes. Except for a 1D spatial discretization (applied along the *x* direction in this case), the method is exact. The MoL formulation used in this study is detailed in,[16] and its application to the modeling of waveguiding structures such as those of concern in this paper is summarized in,[11] the formulation will therefore not be repeated here.

The MoL generates mode solutions that satisfy Eqs. (2) and (3). Since the structures under consideration are invariant along the propagation axis (taken to be in the $+z$ direction), the mode fields vary along this dimension according to $e^{-\gamma z}$ where $\gamma=\alpha+j\beta$ is the complex propagation constant of the mode, αbeing its attenuation constant and β its phase constant. The spatial distribution of all six field components related to a mode can also be generated by the MoL over the 2D cross-section of the structure if they are desired.

The physical symmetry of the structure along the center vertical axis is exploited to increase the accuracy of the results and to reduce the numerical effort required to generate

the mode solutions. This is achieved by placing either an electric wall ($E_{\tan}=0$) or a magnetic wall ($H_{\tan}=0$) boundary condition along the y axis shown in Fig. 1. The top and bottom boundary conditions are placed at infinity and the remaining lateral boundary condition is either placed far enough from the guide to have a negligible effect on the mode calculation, or a lateral absorbing boundary condition is used to simulate infinite space, depending on the level of confinement observed in the resulting mode.

As discussed in Ref. 11, the propagation constant of a mode computed using the method of lines converges in a monotonic or smooth manner with a reduction in the discretization interval, which means that it is sensible to apply an extrapolation technique to generate more accurate values for the propagation constant.[17] The convergence of the computed propagation constants has been monitored during the entire study and extrapolated values obtained using Richardson's extrapolation formula,[18] are used to generate most of the graphs.

C. Modes guided by metal film slab waveguides

As is well known, only two purely bound TM surface modes, each having three field components, are guided by an infinitely wide metal film waveguide.[5] In the plane perpendicular to the direction of wave propagation, the electric field of the modes is comprised of a single component, normal to the interfaces and having either a symmetric or asymmetric spatial distribution across the waveguide. The symmetric mode can have a small attenuation constant and is often termed a long-range surface plasmon-polariton. The fields related to the asymmetric mode penetrate more into the metal than the fields associated with the symmetric mode and are usually much lossier by comparison. In addition to purely bound modes, leaky modes are also known to be supported by these structures.

In the symmetric metal slab structure ($w=\infty$ and $\epsilon_3=\epsilon_1$ in Fig. 1), the spatial distribution of the mode fields is truly symmetric or asymmetric about the horizontal axis passing through the center of the metal film; that is, the fields can be generated by placing a wall of symmetry along this axis. In this structure, the loss associated with the asymmetric mode increases with decreasing film thickness as the fields penetrate progressively deeper into the lossy metal. In the case of the symmetric mode, the attenuation decreases with decreasing film thickness, as the mode evolves towards the transverse electromagnetic (TEM) wave supported by the background. There is no cutoff thickness for either mode in this structure. As the thickness of the film increases, both the symmetric and asymmetric modes become degenerate, their propagation constants converging to that of a plasmon–polariton mode supported by the interface between semi-infinite metallic and dielectric regions, which is given via the following equations:[5]

$$\beta/\beta_0=\mathrm{Re}\left\{\sqrt{\frac{\epsilon_{r,1}\epsilon_{r,2}}{\epsilon_{r,1}+\epsilon_{r,2}}}\right\}, \tag{4}$$

$$\alpha/\beta_0=-\mathrm{Im}\left\{\sqrt{\frac{\epsilon_{r,1}\epsilon_{r,2}}{\epsilon_{r,1}+\epsilon_{r,2}}}\right\}, \tag{5}$$

where $\beta_0=\omega/c_0$ with c_0 being the velocity of light in free space, and $\epsilon_{r,1}$ and $\epsilon_{r,2}$ are the complex relative permittivities of the materials.

In the asymmetric metal slab structure ($w=\infty$ and $\epsilon_3\neq\epsilon_1$ in Fig. 1), the spatial distribution of the mode fields is not truly symmetric or asymmetric about the center horizontal axis. Rather, the distributions are symmetric-like or asymmetric-like; that is the distributions have the general form of those found in the symmetric structure but the fields are localized near one of the interfaces. The modes, however, are still called symmetric and asymmetric modes. The symmetric mode field distribution has a maximum at the interface with the dielectric of lowest permittivity while the asymmetric mode has a maximum at the interface with the dielectric of highest permittivity. The loss associated with the asymmetric mode increases with decreasing film thickness and this mode does not have a cutoff thickness. The loss associated with the symmetric mode decreases with decreasing film thickness and a cutoff thickness for the mode exists; that is, the mode is not supported for films of thickness less than a cutoff value. It is reasonable that a cutoff thickness for the symmetric mode exists in an asymmetric structure since the mode cannot evolve into a TEM wave supported by the background as $t\rightarrow 0$. The background is comprised of the interface between semi-infinite dielectric media and such an interface cannot support a TEM mode. As the thickness of the metal film increases, the modes of the asymmetric structure evolve into uncoupled plasmon-polariton modes supported by the isolated top and bottom interfaces. The propagation constant of the mode localized at the bottom interface converges to the value given by Eqs. (4) and (5) and the propagation constant of the mode localized at the top interface is given by these same equations by substituting ϵ_1 with ϵ_3.

The widely accepted nomenclature for identifying the modes of infinitely wide structures consists in using the letters a or s for asymmetric or symmetric transverse field distributions, respectively, followed by a subscript b or l for bound or leaky modes, respectively. This nomenclature is used for the modes of symmetric as well as asymmetric metal slab structures.

D. Modes guided by metal films of finite width embedded in a homogeneous dielectric

The purely bound modes supported by a thin lossy metal film of finite width, embedded in an infinite homogeneous dielectric ($\epsilon_3=\epsilon_1$ in Fig. 1) have recently been characterized.[11] The modes supported by such structures are not TM in nature but if the structure has an aspect ratio $w/t>1$, then the E_y field component dominates. The modes can be divided into four families depending on the symmetry of their fields. Four symmetries, corresponding to the four possible combinations of electric and magnetic walls placed along the center horizontal and vertical axes, exist and define the families. A mode nomenclature, based on the one used to

identify modes in metal slab waveguides, describes the spatial distribution of the main transverse electric field component, which is the E_y component in most structures of practical interest. A pair of letters *a* or *s* identify whether the main transverse electric field component is asymmetric or symmetric with respect to the *y* and *x* axes, respectively. A superscript is then used to track the number of extrema observed in the spatial distribution of this field component along the largest dimension (usually along the *x* axis) between the corners. A second superscript *n* could be added to track the extrema along the other dimension (the *y* axis) if modes exhibiting them are found. Finally, a subscript *b* or *l* is used to identify whether the mode is bound or leaky. Leaky modes are known to exist in metal film slab structures and though we have yet to search for them in metal films of finite width, their existence is anticipated. The ss_b^0, sa_b^0, as_b^0, and aa_b^0 modes are the first modes supported (one for each of the four possible quarter-symmetries) and thus may be considered as the fundamental modes. In addition to the four fundamental modes, higher-order modes having additional variations in the spatial distribution of their mode fields are supported.

The dispersion of all modes with film thickness is in general consistent with the behavior observed for the purely bound modes supported by the metal film slab waveguide. In addition, one of the fundamental modes and some higher order modes have cutoff thicknesses. The higher order modes have a cutoff width, below which they are no longer propagated. The effect on the modes of varying the background permittivity is consistent with the general behavior observed for the modes supported by a metal film slab waveguide. In addition, the cutoff width of the higher order modes decreases with decreasing background permittivity while all cutoff thicknesses increase.

One of the fundamental modes supported by the symmetric structure, the ss_b^0 mode exhibits very interesting characteristics. This mode evolves with decreasing film thickness towards the TEM wave supported by the background, (an evolution similar to that exhibited by the s_b mode in metal film slab waveguides), its losses and phase constant tending asymptotically towards those of the TEM wave. In addition, decreasing the film width reduces the losses below those of the s_b mode supported by the corresponding metal film slab waveguide. Reducing the background permittivity further reduces the losses. However, a reduction in losses is always accompanied by a reduction in field confinement to the waveguide core which means that attenuation and confinement must be traded-off one against the other. The mode evolved into its most useful form, has a field distribution that renders it excitable using end-fire techniques.[19] Plasmon-polariton waves supported by thin metal films of finite width have recently been observed experimentally at optical communications wavelengths using this method of excitation.[12]

III. MODE CHARACTERISTICS AND EVOLUTION WITH FILM THICKNESS: SMALL ASYMMETRY

A. Mode solutions for a metal film slab waveguide

The study begins with the reproduction of results for an infinitely wide asymmetric metal film waveguide, as shown in Fig. 1 with $w=\infty$, taken from the standard work on such structures.[5] In order to remain consistent with their results, the optical free-space wavelength of excitation is set to $\lambda_0 = 0.633\,\mu$m and their value for the relative permittivity of the silver film at this wavelength is used: $\epsilon_{r,2} = -19 - j0.53$. The relative permittivity of the bottom and top dielectric regions are set to $\epsilon_{r,1}=4$ $(n_1=2)$ and $\epsilon_{r,3} = 3.61$ $(n_3=1.9)$; these values create a structure having a small asymmetry with respect to the horizontal dimension $(\epsilon_1 \approx \epsilon_3)$.

The dispersion curves of the s_b and a_b modes supported by the infinitely wide structure were computed using the MoL and the results are shown in Fig. 2. From this figure, it is seen that the propagation constant of the a_b mode tends towards that of the plasmon-polariton mode supported by the bottom interface, given by Eqs. (4) and (5), as the thickness of the film increases. It is also noted that this mode does not exhibit a cutoff thickness while it is clear that the s_b mode has one near $t=18$ nm. The propagation constant of the s_b mode is seen to tend towards the value of a plasmon-polariton mode supported by the top interface as the thickness increases. These results are in perfect agreement with those reported in.[5]

B. Modes supported by a metal film of width $w=1\,\mu$m

The study proceeds with the analysis of the structure shown in Fig. 1 for the case $w=1\,\mu$m. The material parameters and free-space wavelength that were used in the previous case $(w=\infty)$ were also used here. The dispersion curves for the first seven modes were computed using the MoL and the results are shown in Fig. 2.

In this asymmetric structure, true field symmetry exists only with respect to the *y* axis. With respect to the horizontal dimension, the modes have a symmetric-like or asymmetric-like field distribution with field localization along either the bottom or top metal-dielectric interface. The modes that have a symmetric-like distribution with respect to the horizontal dimension are localized along the metal-dielectric interface with the lowest dielectric constant, while modes that have an asymmetric-like distribution with respect to this axis are localized along the metal-dielectric interface with the highest dielectric constant. This behavior is consistent with that observed for asymmetric metal slab waveguides.

The mode nomenclature adopted for symmetric structures[11] can be used without ambiguity to describe the modes supported by asymmetric structures as long as the modes are identified when the metal film is optically thick, before significant coupling begins to occur through the metal film, and while the origin of the mode can be identified unambiguously. As the metal film thickness decreases, the modes (and their fields) can evolve and change considerably more in an asymmetric structure compared to a symmetric one. The number of extrema in the main transverse electric field component of the mode is counted along the lateral dimension at the interface where the fields are *localized*.

This number is then used in the mode nomenclature. It was observed in[11] that the modes supported by a metal film of finite width are in fact supermodes created from a cou-

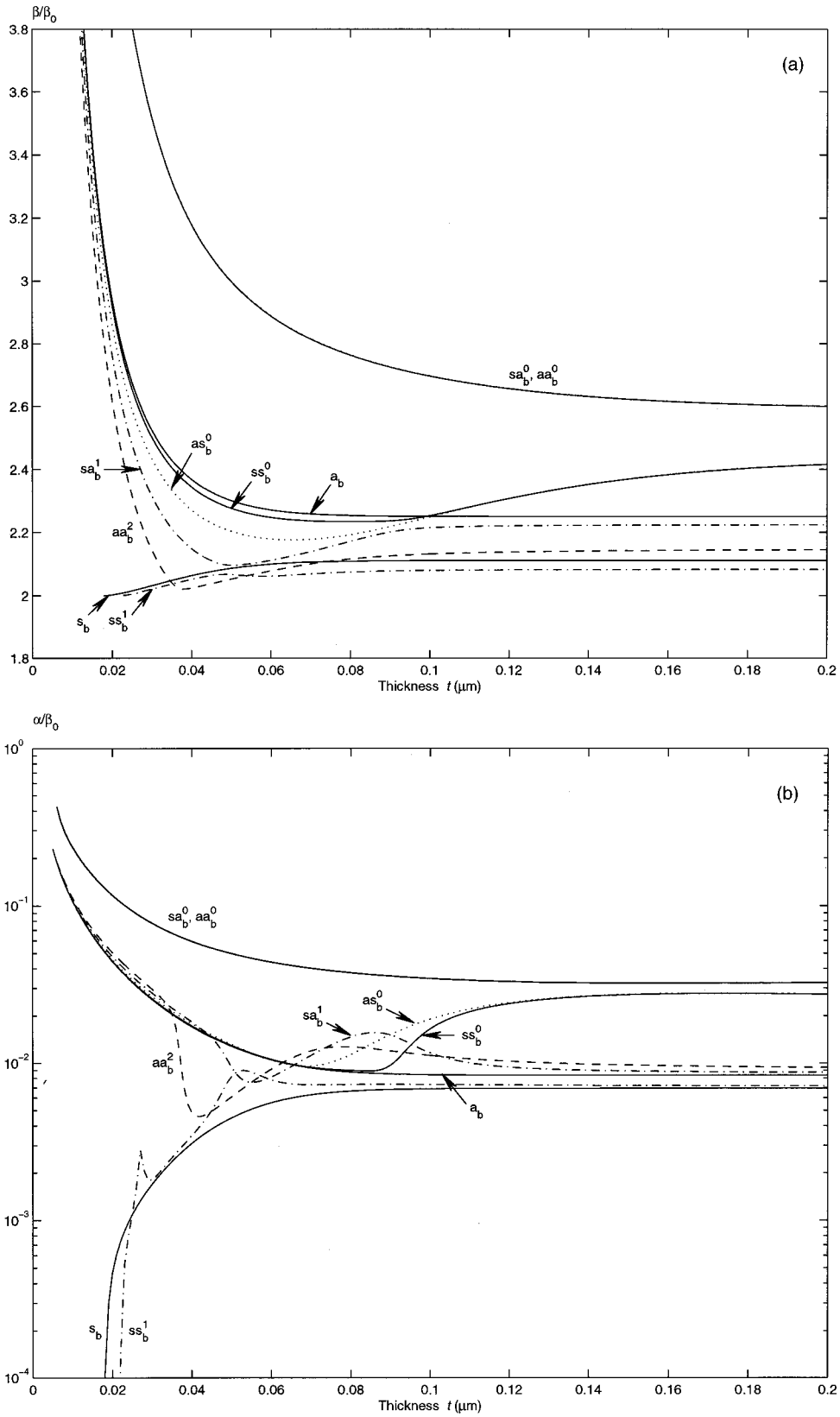

FIG. 2. Dispersion characteristics with thickness of the first seven modes supported by a metal film waveguide of width $w=1$ μm. The a_b and s_b modes supported for the case $w=\infty$ are shown for comparison. (a) Normalized phase constant. (b) Normalized attenuation constant.

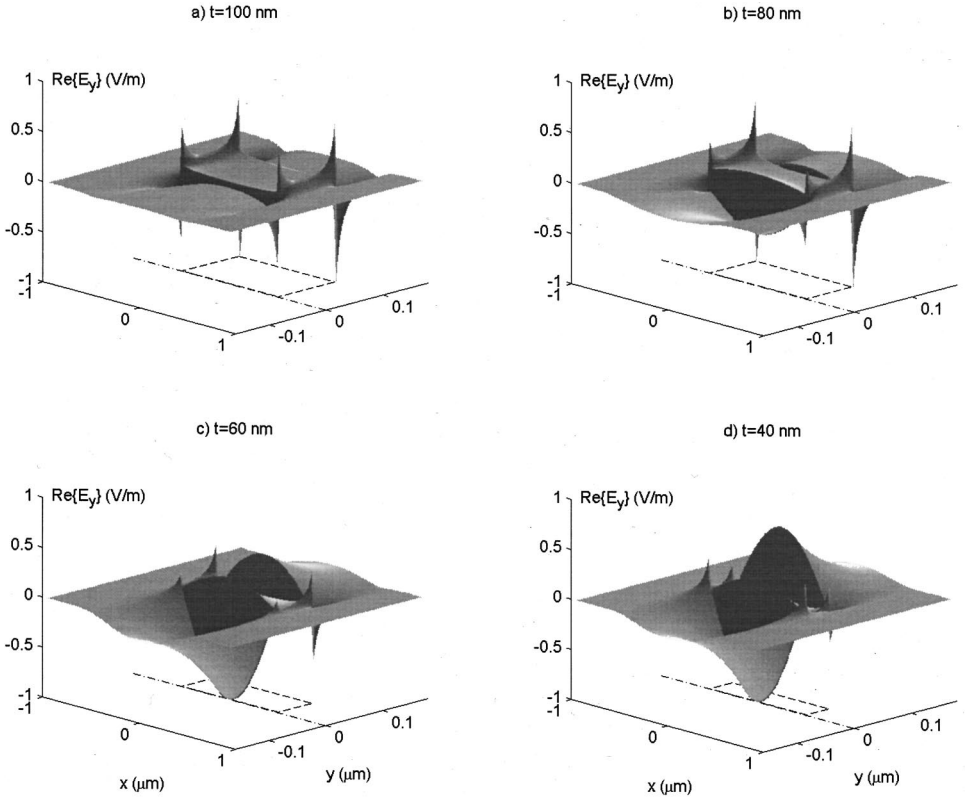

FIG. 3. Spatial distribution of the E_y field component related to the ss_b^0 mode supported by a metal film waveguide of width $w=1\ \mu$m for four film thicknesses. The waveguide cross section is located in the x-y plane and the metal region is outlined as the rectangular dashed contour. The field distributions are normalized such that $\max|\mathrm{Re}\{E_y\}|=1$.

pling of ''edge'' and ''corner'' modes supported by each metal-dielectric interface defining the structure. As the thickness and width of the metal decrease, the coupling between these interface modes intensifies leading to dispersion and possibly evolution of the supermode. In asymmetric structures, the bound modes are also supermodes created in a similar manner, except that dissimilar interface modes may couple to each other to create the supermode. For instance, a mode having one field extremum along the top interface (along the top edge bounded by the corners) may couple with a mode having three extrema along the bottom interface. The selection criteria determining which interface modes will couple to create the supermode are a similarity in the value of their propagation constants and a shared field symmetry with respect to the center vertical axis. For all modes supported by an asymmetric structure, an apparent symmetry or asymmetry with respect to the horizontal dimension can still be observed in the corner modes.

The sa_b^0, aa_b^0, ss_b^0, and as_b^0 modes are the fundamental modes supported by the structure. The sa_b^0 and aa_b^0 modes are comprised of coupled corner modes, resembling the corresponding modes in a symmetric structure[11] except that the fields are localized near the substrate. These two modes do not change in character as the thickness of the film decreases. A narrowing of the metal film would eventually break the degeneracy observed in Fig. 2.

For a sufficiently large thickness (about 100 nm for the present structure), the ss_b^0 and as_b^0 modes are comprised of coupled corner modes much like the corresponding modes in a symmetric structure except that the fields are localized near the superstrate. As the thickness of the metal film decreases, both of these modes begin to evolve, changing completely in character for very thin films. Figure 3 shows the evolution of the E_y field component related to the ss_b^0 mode as the thickness of the film ranges from 100 to 40 nm. It is clearly seen that the mode evolves from a symmetric-like mode having fields localized near the superstrate to an asymmetric-like mode having fields localized along the substrate-metal interface. A similar evolution is observed for the as_b^0 mode. This change in character is also apparent in their dispersion curves: they follow the general behavior of a symmetric-like mode for large thicknesses but then slowly change to follow the behavior of an asymmetric-like mode as the thickness decreases. Since the substrate dielectric constant is larger than the superstrate dielectric constant, the mode is ''pulled'' from a symmetric-like mode to an asymmetric-like mode (having field localization at the substrate-metal interface) as the metal film becomes thinner. The behavior of these modes as the film thickness decreases is quite unexpected, differing completely from their behavior in a symmetric structure. In the latter, they exhibit a decreasing attenuation with decreasing film thickness, the ss_b^0 is the main long-ranging mode and the as_b^0 mode has a cutoff thickness.[11] In this asymmetric structure both modes exhibit an increasing attenuation with decreasing thickness and the as_b^0 mode does not have a cutoff thickness.

Figure 4 shows the E_y field component related to the ss_b^1 and sa_b^1 modes for two film thicknesses. From this figure it is noted that the top and bottom edge modes comprising a supermode are different from each other. In Fig. 4(a) for instance, it is seen that the bottom edge mode has three extrema and is of higher order than the top edge mode which has one extremum. A similar observation holds for Fig. 4(c)

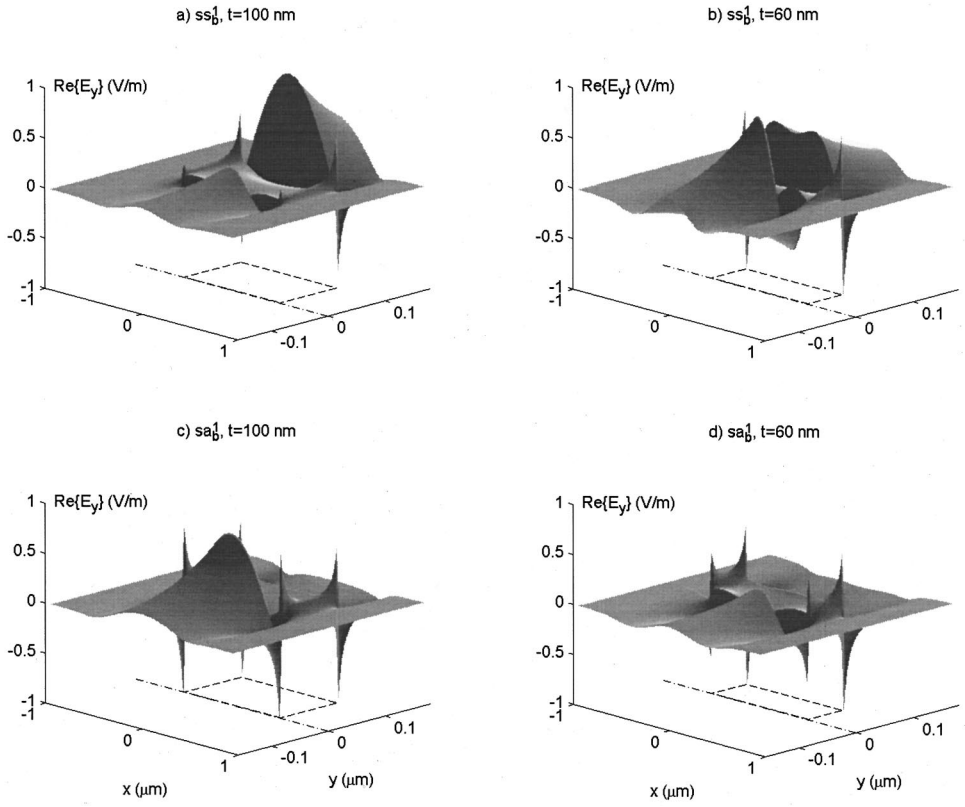

FIG. 4. Spatial distribution of the E_y field component related to two higher-order modes supported by a metal film waveguide of width $w=1\ \mu$m for two film thicknesses. In all cases, the waveguide cross section is located in the x-y plane and the metal region is outlined as the rectangular dashed contour. The field distributions are normalized such that $\max|\mathrm{Re}\{E_y\}|=1$.

where it can be seen that the bottom edge mode has one extremum while the top one has none. In this structure, the substrate has a higher dielectric constant than the superstrate so the phase constant of a particular substrate–metal interface mode will be higher than the phase constant of the same mode at the metal–superstrate interface. Since a supermode is created from a coupling of edge modes having similar propagation constants, it should be expected that in an asymmetric structure different edge modes may couple to create a supermode. Higher-order modes have, in general, smaller values of phase constant compared to lower-order modes, so in structures having $\epsilon_3<\epsilon_1$, all supermodes are comprised of a bottom edge mode of the same order or higher than the top edge mode, as shown in Fig. 4. If $\epsilon_3>\epsilon_1$, then the opposite statement is true.

A careful inspection of the fields associated with the ss_b^1, sa_b^1, and aa_b^2 modes reveals that as the thickness of the film decreases, the mode fields may evolve in a smooth manner similar to that shown in Fig. 3, but in addition a change or ''switch'' of the constituent edge modes may also occur. For instance, from Fig. 4(c), the sa_b^1 mode is seen to be comprised of a substrate–metal interface mode having one extremum for a film thickness of 100 nm, while for a thickness of 60 nm the substrate–metal interface mode has three extrema, as shown in Fig. 4(d). Since higher-order modes have, in general, lower phase constants than lower-order modes, this change in edge modes causes a reduction in the phase constant of the sa_b^1 mode in the neighborhood of 60 nm, as shown in Fig. 2(a). Another change occurs near 40 nm as the corner modes switch from being symmetric-like [as in parts (c) and (d) of Fig. 4] to being asymmetric-like with respect to the horizontal dimension. This change is again reflected in the dispersion curve of the sa_b^1 mode as its phase constant is seen to increase with a further decrease in thickness. In general, the changes in the edge and corner modes are consistent with the directions taken by the dispersion curves as the film thickness decreases, thus explaining the strange appearance of the curves shown in Fig. 2.

The only potentially long-ranging mode supported by this structure at the wavelength of analysis is the ss_b^1 mode. As shown in Fig. 2, the mode has a cutoff thickness near $t=22$ nm and though the attenuation drops quickly near this thickness, it should be remembered that the field confinement does so as well. Furthermore, the spatial distribution of the main transverse field component related to this mode evolves with decreasing thickness in the manner shown in Figs. 4(a) and 4(b), such that near cutoff the spatial distribution has strong extrema along the top and bottom edges. These extrema render the mode less excitable using an end-fire technique so coupling losses would be higher compared to the fundamental symmetric mode in symmetric waveguides. Also, the fact that the mode would be operated near its cutoff thickness implies that very tight tolerances are required in the fabrication of structures. Nevertheless, it should be possible to observe propagation of this mode in a suitable structure in an end-fire experiment.

IV. MODE CHARACTERISTICS AND EVOLUTION WITH FILM THICKNESS: LARGE ASYMMETRY

A. Mode solutions for a metal film slab waveguide

The study proceeds with the analysis of structures having a large difference in the dielectric constants of the substrate

and superstrate. With respect to Fig. 1, the relative permittivity of the substrate and superstrate are set to $\epsilon_{r,1}=4$ $(n_1=2)$ and $\epsilon_{r,3}=2.25$ $(n_3=1.5)$, respectively, the width of the metal film is set to $w=\infty$, and the dielectric constant of the metal region and the wavelength of analysis are set to the same values as in the previous section. The dispersion curves of the s_b and a_b modes supported by this structure have been computed using the MoL and are shown in Fig. 5. Comparing with Fig. 2, it is observed that the s_b mode has a larger cutoff thickness in a structure having a large asymmetry than in a structure having similar substrate and superstrate dielectric constants. The results are in perfect agreement with those reported in.[5]

B. Modes supported by a metal film of width $w=1\ \mu$m

The structure shown in Fig. 1 was analyzed using the MoL for $w=1\ \mu$m and for the same material parameters and free-space wavelength as those given above for $w=\infty$. The dispersion curves of the first six modes supported by the structure are shown in Fig. 5.

An inspection of the mode fields related to the sa_b^0 and aa_b^0 modes reveals that these modes are again comprised of coupled corner modes with fields localized at the substrate–metal interface. The modes do not change in character as the thickness of the film decreases and a narrowing of the metal film would eventually break the degeneracy observed in Fig. 5.

The spatial distribution of the E_y field component related to the ss_b^0, as_b^0, sa_b^1, and aa_b^2 modes is given in Fig. 6. It is noted from this figure that in all cases the metal–superstrate interface modes are similar: they have fields with no extrema along the interface but rather that are localized near the corners and have either a symmetric or asymmetric distribution with respect to the y axis. These corner modes are, in fact, the lowest-order modes supported by the metal–superstrate interface; they have the largest value of phase constant and thus are most likely to couple with edge modes supported by the substrate–metal interface to form a supermode. From Figs. 6(a) and 6(b), it is observed that the substrate–metal interface modes comprising the ss_b^0 and as_b^0 modes are of very high order. This is expected since the substrate dielectric constant is significantly higher than the superstrate dielectric constant and higher order modes have lower values of phase constant. The ss_b^0 and as_b^0 modes shown in Figs. 6(a) and 6(b) indeed have fields that are localized along the metal–superstrate interface, while the sa_b^1 and aa_b^2 modes shown in Figs. 6(c) and 6(d) have fields that are localized along the substrate-metal interface.

One effect caused by increasing the difference between the substrate and superstrate dielectric constants, is that the difference between the orders of the top and bottom edge modes comprising a supermode can increase. This effect can be observed by comparing Fig. 3(a) with Fig. 6(a). In the former, there is no difference between the orders of the top and bottom edge modes, while in the latter the difference in the orders is 5. Another effect is that the degree of field localization increases near the interface between the metal and the dielectric of higher permittivity, for all modes that are asymmetric-like with respect to the horizontal dimension. This effect can be seen by comparing the fields related to the sa_b^1 mode shown in Figures 4(c) and 6(c). A comparison of the fields related to the sa_b^0 and aa_b^0 modes reveals that this effect is present in these modes as well.

From the dispersion curves shown in Fig. 5(a), it is apparent that the normalized phase constant of all modes converge with increasing film thickness to normalized phase constants in the neighborhood of those supported by plasmon–polariton waves localized along the associated isolated edge. The normalized phase constant of modes having fields localized at the substrate-metal interface, converge with increasing film thickness to normalized phase constants in the neighborhood of that related to the a_b mode, while the normalized phase constant of modes having fields localized along the metal-superstrate interface converge to values near that of the s_b mode. This behavior is present though less apparent in structures where the asymmetry is smaller, such as the one analyzed in Sec. III.

By comparing Figs. 2 and 5, it is noted that the dispersion curves of the modes are much smoother in this case, where the difference in the substrate and superstrate dielectric constants is large. This is due to the fact that the edge modes comprising the supermodes are less likely to change or switch as they do in a structure having similar substrate and superstrate dielectric constants. Modes that start out being symmetriclike with respect to the horizontal dimension remain so as the thickness of the film decreases since the phase constant associated with the interface modes localized along the substrate-metal interface are much larger. The cutoff thickness of the symmetriclike modes also increases as the difference between the substrate and superstrate dielectric constants increases. It is surprising in this case that the ss_b^0 mode has a larger cutoff thickness than the as_b^0 mode.

It is apparent that introducing a large asymmetry can hamper the ability of the structure to support useful long-ranging modes. Any mode that is long-ranging in such structures would likely have fields with numerous extrema along the width of the interface between the metal film and the dielectric of higher permittivity, as shown in Figs. 6(a) and 6(b).

V. MODE DISPERSION WITH FILM WIDTH: SMALL ASYMMETRY

An asymmetric structure comprised of the same dielectrics as the structures studied in Sec. III, but having a metal film of width $w=0.5\ \mu$m was analyzed at the same free-space wavelength in order to determine the impact of a narrowing film width on the modes supported. The structure was analyzed using the MoL and Fig. 7 gives the dispersion curves obtained for the first few modes supported.

Comparing Fig. 7 with Fig. 2 reveals that reducing the width of the film does not cause major changes in the behavior of the fundamental modes, but does have a major impact on the higher order modes. It is noted that reducing the film width increases the cutoff thickness of the ss_b^1 mode. This higher-order mode is symmetric-like with respect to the horizontal dimension, and the cutoff thickness of the symmetric-

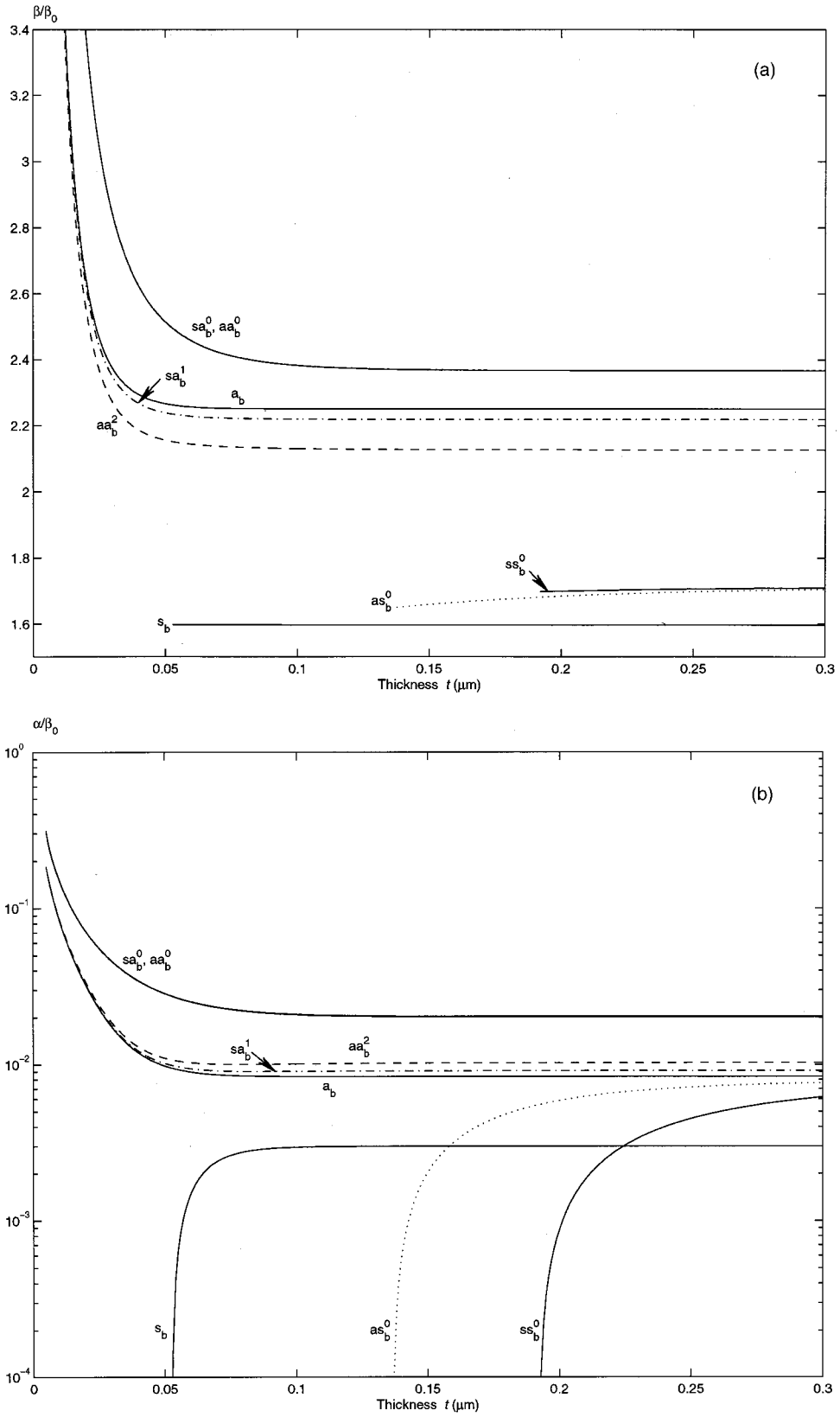

FIG. 5. Dispersion characteristics with thickness of the first six modes supported by a metal film waveguide of width $w=1$ μm. The a_b and s_b modes supported for the case $w=\infty$ are shown for comparison. (a) Normalized phase constant. (b) Normalized attenuation constant.

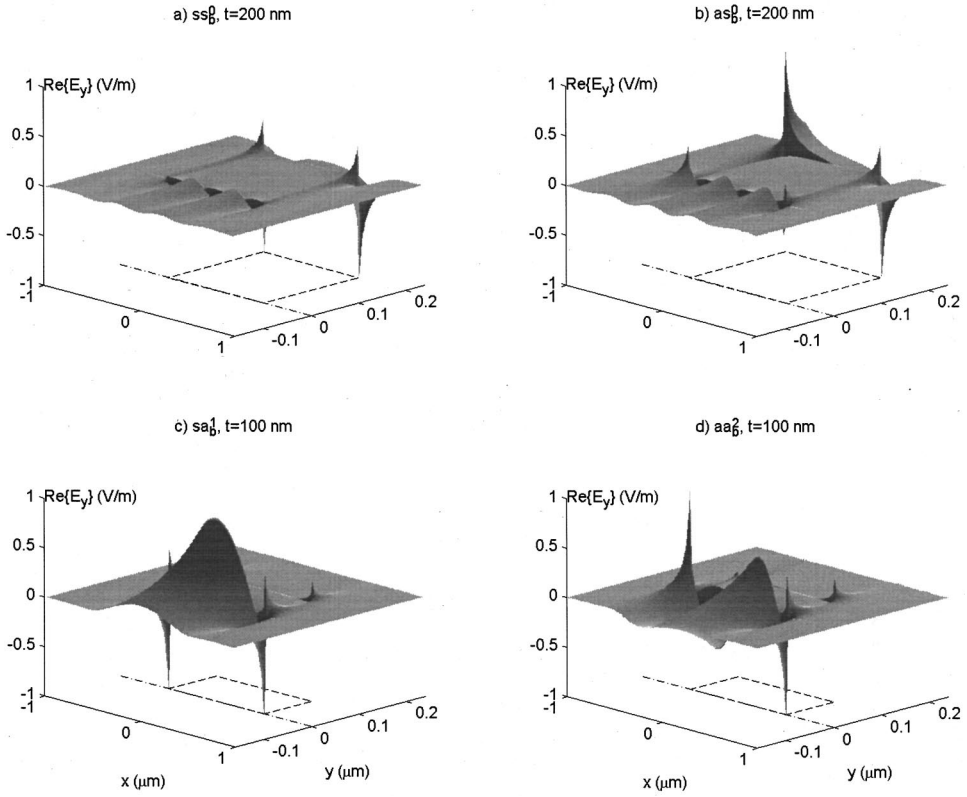

FIG. 6. Spatial distribution of the E_y field component related to modes supported by a metal film waveguide of width $w=1\ \mu$m. In all cases, the waveguide cross section is located in the x-y plane and the metal region is outlined as the rectangular dashed contour. The field distributions are normalized such that $\max|\mathrm{Re}\{E_y\}|=1$.

like modes, in general, increases as the width of the film decreases due to a reduction in field confinement to the metal film. The aa_b^2 mode was sought but not found for this film width.

It is also noted by comparing Figs. 7 and 2 that the sa_b^1 mode evolves quite differently depending on the width of the film. For a film width of $w=1\ \mu$m, the mode follows the general behavior of an asymmetriclike mode whereas for a film width of $w=0.5\ \mu$m, the mode evolves as a symmetriclike mode, and has a cutoff thickness near $t=27$ nm. When the film is wide, it becomes possible for numerous higher order edge modes (having similar values of phase constant) to be supported by the substrate–metal or metal–superstrate interfaces, so edge modes comprising a supermode are likely to change or switch as the thickness of the film is reduced as shown in Figs. 4(c) and 4(d). For a narrow metal film, some of the higher-order edge modes may be cutoff thus rendering changes in edge modes impossible. In such a case, the supermode may be forced to evolve in a smooth manner with decreasing film thickness. A close inspection of the mode fields related to the sa_b^1 mode for a film width of $w=0.5\ \mu$m reveals that there are no changes to the edge modes as the thickness decreases, rather the mode evolves smoothly from its field distribution at a large thickness [similar to that shown in Fig. 4(c)] to having a symmetric-like distribution with only one extremum along the top and bottom edges of the film.

For structures comprised of a thin narrow metal film in a slightly asymmetric environment, the main long-ranging mode is the sa_b^1 mode, and it could be made to propagate over useful distances if it is excited near its cutoff thickness. However, the difficulties outlined previously regarding the excitation of modes near cutoff still hold.

VI. EVOLUTION OF THE LONG-RANGING MODE WITH STRUCTURE ASYMMETRY

The ss_b^0 and sa_b^1 modes are of practical interest. The ss_b^0 mode is the main long-ranging mode supported by symmetric finite-width metal film structures, and as demonstrated in the previous section, the sa_b^1 mode can be the main long-ranging mode supported by asymmetric finite-width structures. In metal films of the right thickness, they are also the modes that are the most suitable to excitation in an end-fire arrangement.

Structures comprised of a substrate dielectric having $n_1=2$, of a metal film of width $w=0.5\ \mu$m, and of various superstrate dielectrics having $n_3=2$, 1.99, 1.95, and 1.9 were analyzed at the same free-space wavelength as in the previous sections, and using the same equivalent permittivity for the metal film. The analyses were performed in order to investigate the effects on the propagation characteristics of the ss_b^0 and sa_b^1 modes caused by a slight decrease in the superstrate permittivity relative to the substrate permittivity. Figure 8 shows the dispersion curves with film thickness, obtained for these modes in the four structures of interest; the insets show an enlarged view of the intersection region.

As seen in Fig. 8(a) and its inset, the dispersion curves of the modes intersect at a certain film thickness only for the symmetric case ($n_3=n_1$). As soon as some degree of asymmetry exists, the curves no longer intersect, though they may come quite close to each other if the asymmetry is small, as seen in the case of $n_3=1.99$. As the degree of asymmetry increases, the separation between the curves increases.

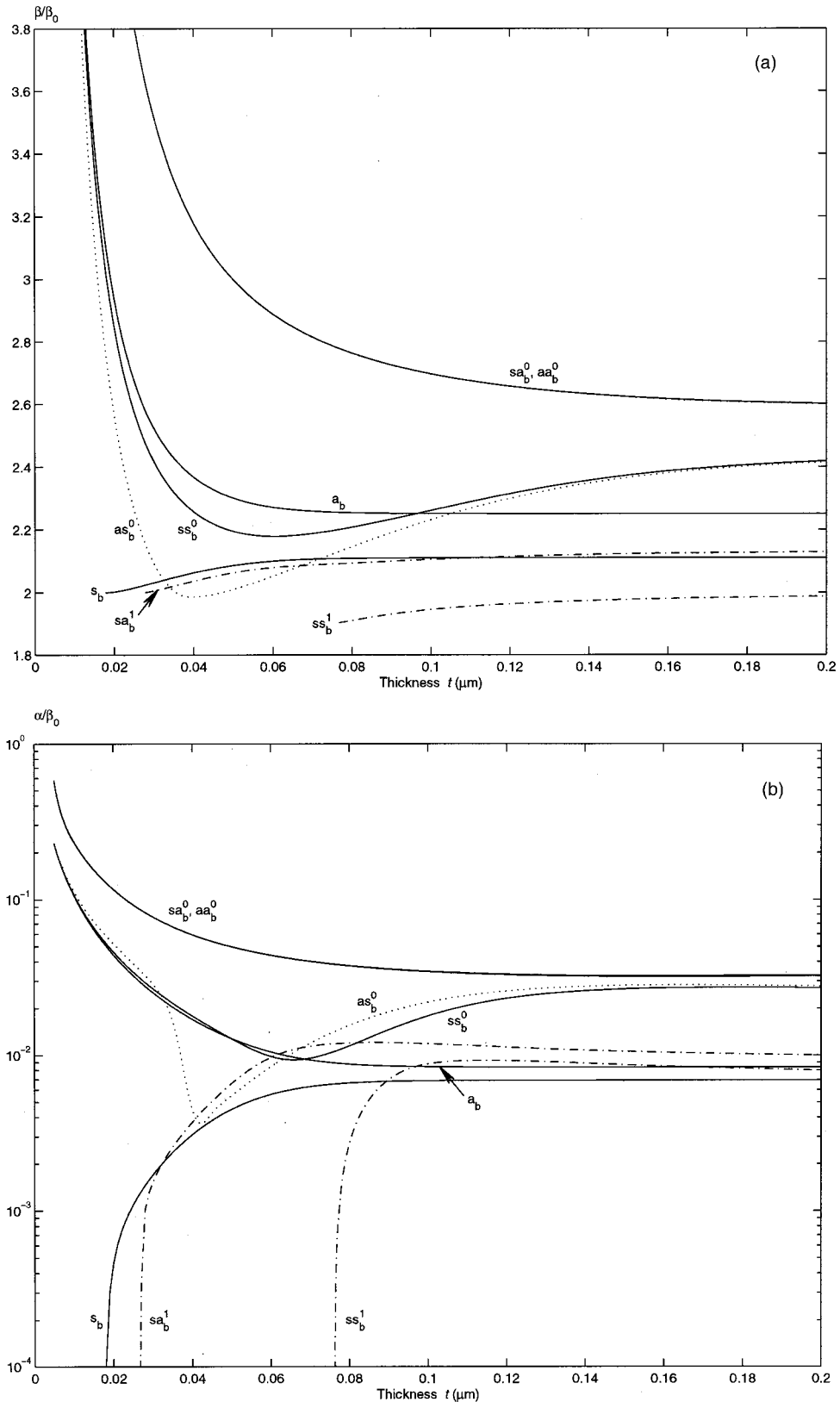

FIG. 7. Dispersion characteristics with thickness of the first six modes supported by a metal film waveguide of width $w=0.5\,\mu$m. The a_b and s_b modes supported for the case $w=\infty$ are shown for comparison. (a) Normalized phase constant. (b) Normalized attenuation constant.

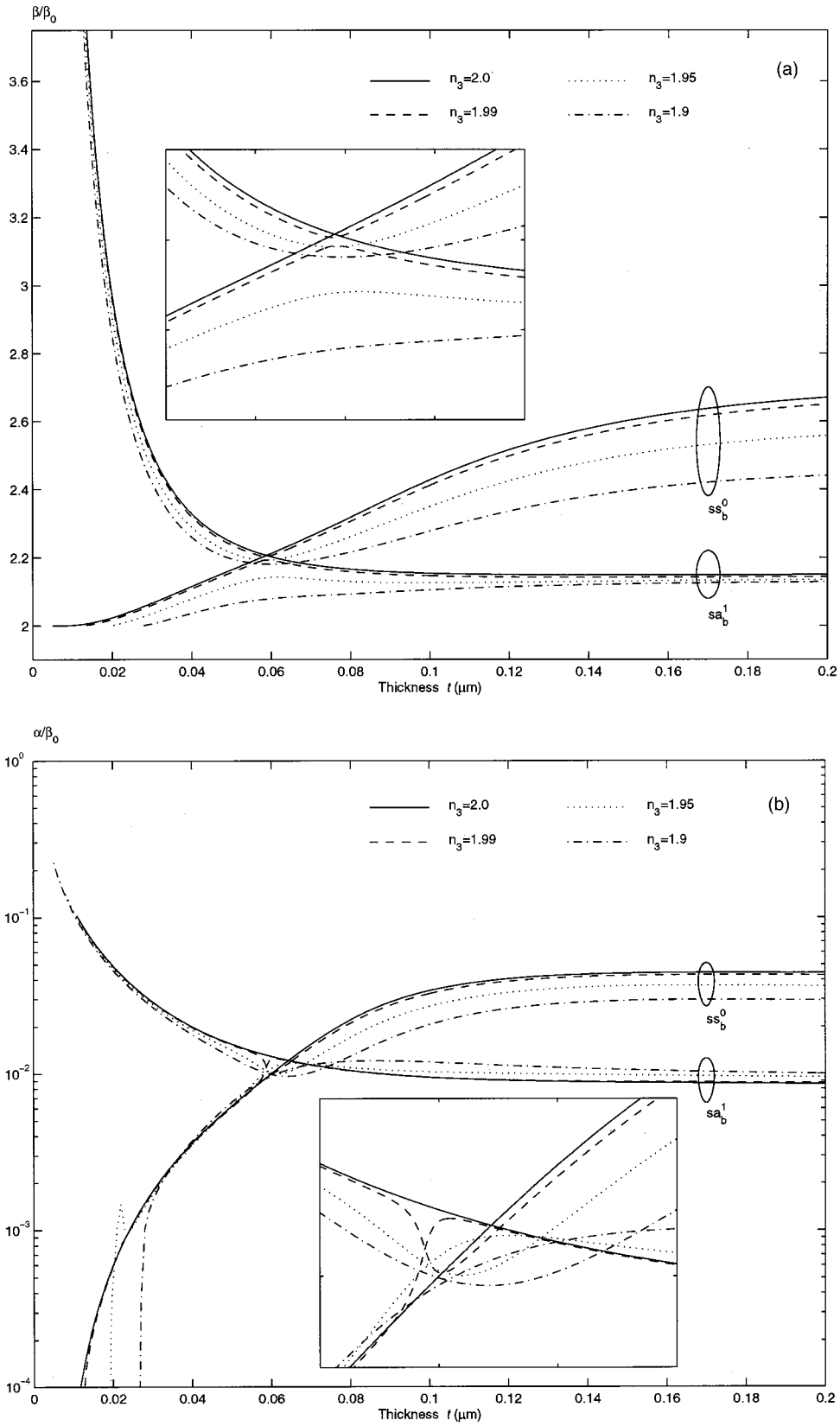

FIG. 8. Dispersion characteristics with thickness of the ss_b^0 and sa_b^1 modes supported by a metal film waveguide of width $w=0.5\ \mu$m for various cases of ϵ_3. (a) Normalized phase constant; the inset shows an enlarged view of the region bounded by $0.04 \leqslant t \leqslant 0.08\ \mu$m and $2.0 \leqslant \beta/\beta_0 \leqslant 2.3$. (b) Normalized attenuation constant; the inset shows an enlarged view of the region bounded by $0.05 \leqslant t \leqslant 0.08\ \mu$m and $7.0\times10^{-3} \leqslant \alpha/\beta_0 \leqslant 2.0\times10^{-2}$.

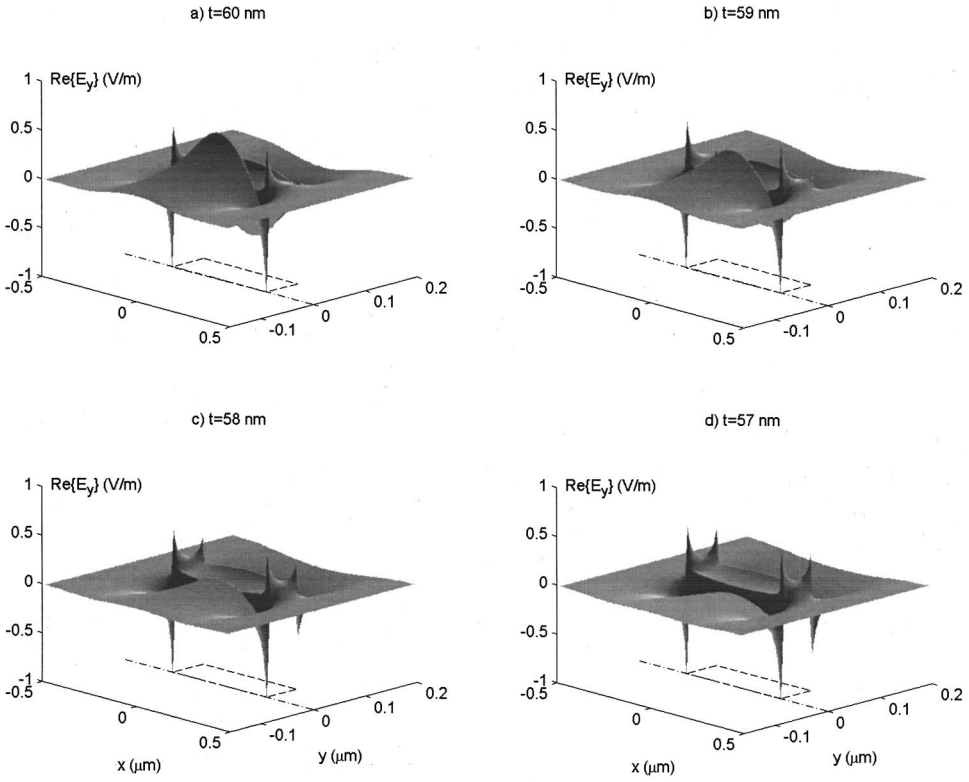

FIG. 9. Spatial distribution of the E_y field component related to the sa_b^1 mode supported by a metal film waveguide of width $w=0.5\,\mu$m for four film thicknesses. The waveguide cross section is located in the x-y plane and the metal region is outlined as the rectangular dashed contour. The field distributions are normalized such that $\max|\mathrm{Re}\{E_y\}|=1$.

The evolution with film thickness of the sa_b^1 mode is shown in Fig. 9 for the case $n_3=1.99$ and for thicknesses about $t=59$ nm (near the maximum in its phase dispersion curve). The evolution of this mode for the cases $n_3=1.95$ and 1.9 is similar to that shown. The evolution with film thickness of the ss_b^0 mode is similar in these structures to the evolution shown in Fig. 3 for the case $w=1\,\mu$m and $n_3=1.9$. Comparing Figs. 9 and 3, reveals that the modes ''swap'' character near $t=59$ nm. For film thicknesses sufficiently above this value, the modes exhibit their defining character, as shown in Figs. 3(a) and 9(a), but for film thicknesses below it, each mode exhibits the other's character, as shown in Figs. 3(d) and 9(d). This character swap is present for the three cases of asymmetry considered here ($n_3=1.99$, 1.95, and 1.9) and explains the behavior of the dispersion curves shown in Fig. 8.

From Fig. 8, it is noted that a cutoff thickness exists for the long-ranging mode as soon as an asymmetry is present in the structure. It is also observed that the cutoff thickness increases with increasing asymmetry. Table I gives the cutoff thicknesses of the sa_b^1 mode, and of the s_b mode related to the corresponding slab structures, for these three cases of asymmetry. From this table, it is noted that the cutoff thickness of the sa_b^1 mode is always greater than the cutoff thickness of the s_b mode. This result implies that the long-ranging mode supported by a thin narrow metal film is more sensitive to differences in the superstrate and substrate permittivities than the s_b mode supported by the corresponding slab structure. This is reasonable in light of the fact that in finite-width structures the mode fields tunnel through the metal as in slab structures, but in addition the fields also wrap around the metal film.

It is expected that as the width of the metal film increases, the cutoff thickness of the sa_b^1 mode will decrease as long as the mode remains long ranging. It should be remembered that the character of this mode may change with film width and with the degree of asymmetry such that its behavior becomes similar to that of the a_b mode in the corresponding slab structure, as shown in Fig. 2.

Figure 8(b) shows that near cutoff, the attenuation of the sa_b^1 mode supported by the asymmetric structures drops much more rapidly than the attenuation of the ss_b^0 mode supported by the symmetric one. As in slab waveguides,[6] introducing a slight asymmetry in a structure of finite width appears to be a suitable means for extending the range of the mode.

Figure 10 shows contour plots of $\mathrm{Re}\{S_z\}$ associated with the long-ranging modes for four cases of superstrate permittivity. S_z is the z-directed component of the Poynting vector and its spatial distribution is computed from the spatial distribution of the mode fields using:

TABLE I. Cutoff thickness of the s_b and sa_b^1 modes for six cases of structure asymmetry.

n_3	s_b (nm)	sa_b^1 (nm)
1.99	4.25	12
1.95	10.5	19.2
1.9	17.6	26.7
2.01	4.2	12
2.05	10	18
2.1	15.4	22.3

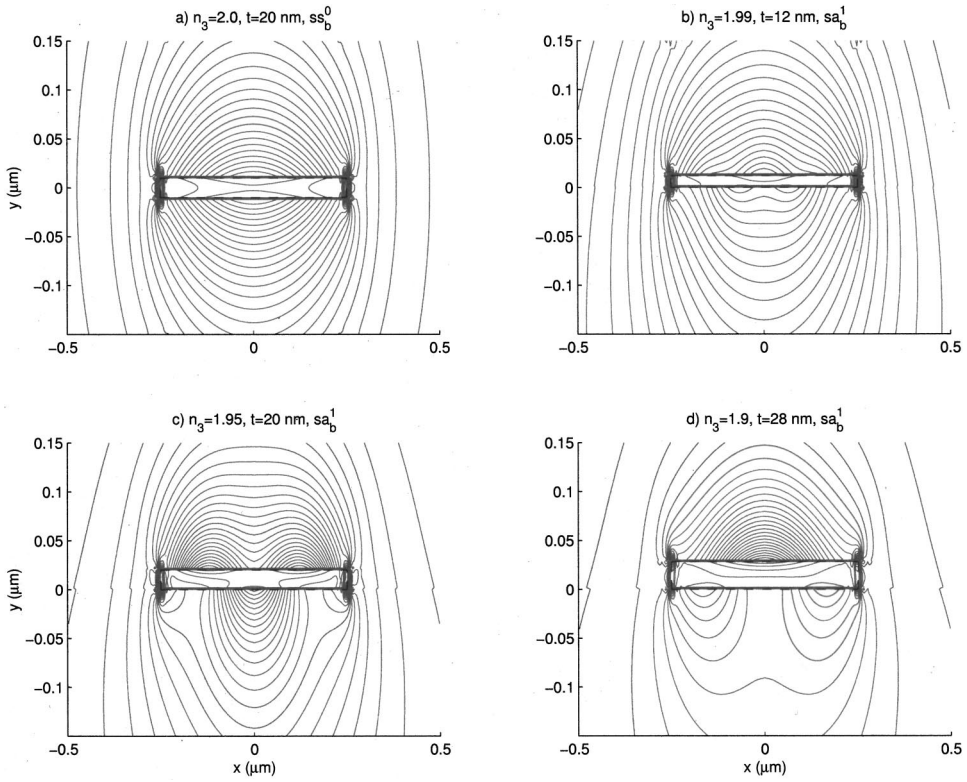

FIG. 10. Contour plot of $\mathrm{Re}\{S_z\}$ associated with the long-ranging modes supported by metal film waveguides of width $w=0.5\,\mu$m and having different superstrate permittivities ϵ_3. In all cases, the outline of the metal film is shown as the rectangular dashed contour.

$$S_z=\frac{1}{2}(E_xH_y^*-E_yH_x^*), \tag{6}$$

where $H_{x,y}^*$ denotes the complex conjugate of $H_{x,y}$. Figure 10(a) shows the contour plot associated with the ss_b^0 mode supported by a symmetric structure ($n_3=n_1=2$) of thickness $t=20$ nm. Figures 10(b)–10(d) show contours associated with the sa_b^1 mode for the three cases of structure asymmetry considered. The contour plots shown in Figs. 10(b)–10(d) are computed for film thicknesses slightly above cutoff, representative of the thicknesses that would be used to observe these long-ranging modes experimentally. From this figure, it is noted that the contour plots become increasingly distorted and the fields increasingly localized at the metal-superstrate interface as the degree of asymmetry in the structure increases. It is also apparent by comparing Figs. 10(a) and 10(d) that in an end-fire experiment, less power would be coupled into the sa_b^1 mode supported by the asymmetric structure with $n_3=1.9$, compared to the ss_b^0 mode supported by the symmetric one since the mode fields would not overlap as cleanly with those of the excitation source. This suggests that end-fire coupling losses increase in general with increasing structure asymmetry.

The high sensitivity of the long-ranging mode, supported by thin metal films of finite width, to structure asymmetry is potentially useful. A small induced asymmetry (created via an electro-optic effect present in the dielectrics say) can evidently affect a large change in the propagation characteristics of the long-ranging mode. From Fig. 8, it is apparent that a difference between the substrate and superstrate refractive indices as small as $n_1-n_3=\Delta n=0.01$ is sufficient to create an asymmetric structure where the long-ranging mode has a cutoff thickness of about $t=12$ nm. From Fig. 8(a), a slightly larger difference of $\Delta n=0.05$ changes the normalized phase constant of the long-ranging mode by $\Delta(\beta/\beta_0)\approx 0.025$ for a metal film thickness of $t=20$ nm. Both of these effects are potentially useful.

Asymmetric structures having superstrate dielectric constants that are slightly greater than that of the substrate were also analyzed. The substrate dielectric constant was set to $n_1=2$ and superstrate dielectrics having $n_3=2.01$, 2.05, and 2.1 were considered for the same metal, film width and operating wavelength. The results are similar to those presented in Figs. 8–10 and the cutoff thicknesses are given in Table I. Though the results are not identical, there is no major difference between the behavior of the ss_b^0 and sa_b^1 modes whether $\epsilon_1>\epsilon_3$ or $\epsilon_1<\epsilon_3$ as long as the permittivities are similar.

VII. CONCLUSION

The purely bound optical modes supported by a thin lossy metal film of finite width, supported by a semi-infinite substrate dielectric and covered by a different semi-infinite superstrate dielectric, have been characterized and described. The modes differ significantly from those supported by corresponding slabs and similar symmetric structures of finite width. In addition to the four fundamental modes that exist, numerous higher-order modes are supported, each having a cutoff width. The dispersion of the modes with film thickness has been assessed and the general behavior found to be rather complex. All modes are eventually divided along symmetric or asymmetric branches as the thickness of the metal film tends toward zero but the dispersion curves can exhibit an unusual oscillatory character. Contrary to symmetric

finite-width metal film structures, all modes that exhibit a decreasing attenuation with film thickness, also have a cutoff thickness. Mode dispersion with film width has been investigated and described. The difference between the substrate and superstrate permittivities has been varied and the effects on the modes have been determined. It has been found that the modes may change dramatically in character as the dimensions of the metal film change and as the difference between the substrate and superstrate permittivities increases. The evolution of the modes is explained in terms of a selective coupling of appropriate edge and corner modes according to the relative similarity of their propagation constants and to a shared symmetry with respect to the center vertical axis.

Under the right conditions, a long-ranging mode can be supported. The mode has a rapidly diminishing attenuation near its cutoff thickness and the rate of decrease of its attenuation with decreasing thickness is greater than the rate related to the ss_b^0 mode in symmetric structures. However the confinement of the mode to the film also diminishes rapidly, implying that the structures ought to be fabricated to very tight tolerances and that all metal-dielectric interfaces should be of the highest quality. Below this cutoff thickness, no purely bound long-ranging mode exists. Also, the mode is more sensitive to the asymmetry in the structure compared to the s_b mode supported by the corresponding slab waveguide. This is a potentially useful result in that a small induced change in substrate or superstrate refractive index can have a greater impact on the long-ranging mode supported by a finite-width structure compared to a similar slab waveguide.

*Fax: (613) 562-5175; E mail: berini@site.uottawa.ca

[1] *American Institute of Physics Handbook*, 3rd ed. (McGraw-Hill, New York, 1972).
[2] *Handbook of Optics* (McGraw-Hill, New York, 1978).
[3] A. D. Boardman, *Electromagnetic Surface Modes*, edited by A. D. Boardman (Wiley Interscience, New York, 1982).
[4] E. N. Economou, Phys. Rev. **182**, 539 (1969).
[5] J. J. Burke, G. I. Stegeman, and T. Tamir, Phys. Rev. B **33**, 5186 (1986).
[6] L. Wendler and R. Haupt, J. Appl. Phys. **59**, 3289 (1986).
[7] F. A. Burton and S. A. Cassidy, J. Lightwave Technol. **8**, 1843 (1990).
[8] F. Yang, J. R. Sambles, and G. W. Bradberrey, Phys. Rev. B **44**, 5855 (1991).
[9] B. Prade, J. Y. Vinet, and A. Mysyrowicz, Phys. Rev. B **44**, 13 556 (1991).
[10] P. Tournois and V. Laude, Opt. Commun. **137**, 41 (1997).
[11] P. Berini, Phys. Rev. B **61**, 10 484 (2000).
[12] R. Charbonneau, P. Berini, E. Berolo, and E. Lisicka-Skrzek, Opt. Lett. **25**, 844 (2000).
[13] W. Johnstone, G. Stewart, T. Hart, and B. Culshaw, J. Lightwave Technol. **8**, 538 (1990).
[14] P. Berini, Opt. Express **7**, 329 (2000).
[15] R. Pregla and W. Pascher, ''The method of lines,'' in *Numerical Techniques for Microwave and Millimeter-Wave Passive Structures*, edited by T. Itoh (Wiley Interscience, New York, 1989).
[16] P. Berini and K. Wu, IEEE Trans. Microwave Theory Tech. **MTT-44**, 749 (1996).
[17] R. Culver, Br. J. Appl. Phys. **3**, 376 (1952).
[18] R. C. Boonton, *Computational Methods for Electromagnetics and Microwaves* (Wiley Interscience, New York, 1992).
[19] G. I. Stegeman, R. F. Wallis, and A. A. Maradudin, Opt. Lett. **8**, 386 (1983).